

Impact Risk Assessment of a Fragmented Asteroid in Earth Resonant Orbits

George Vardaxis* and Bong Wie†

Iowa State University, Ames, IA 50011-2271, USA

Taking advantage of direct numerical simulation, analytic keyhole theory, B-plane mapping, and planetary encounter geometry are shown to be useful in determining the impact probability of an asteroid with the Earth on a given encounter, as well as the potential for future encounters. The accurate estimation of the impact probability of hazardous asteroids is extremely important for space mission planning in order to mitigate their impact threat to Earth. Asteroids in Earth's resonant orbits are particularly troublesome because of the continuous threat they pose in the future. Expanding upon the established theory, a computational method is developed to estimate the impact probability of an asteroid, fragmented into many pieces by a disruption mission, on their current and future encounters with Earth.

I. Introduction

The problem of orbital prediction is not new to the field of celestial or orbital mechanics. The results of the orbital prediction problem could be more important now than ever, however. The threat that Earth faces everyday from asteroids is very real and ever-present. For the case of most impacts, the objects are too small to do any damage on the surface because they burn up in the atmosphere, however, there are the rare few cases where an object does make landfall. The number of identified potentially hazardous near-Earth asteroids is increasing, and so is the likelihood of one of those asteroids posing a non-negligible threat to the planet. The human race is in a unique position to do something about those threats to mitigate and/or eliminate them.

Dealing with the threat of any near-Earth object has three main steps: detection/tracking, characterization, and mitigation. NASA, as well as other organizations, have put a lot of effort into the detection/tracking of all near-Earth objects - threatening and non-threatening. At the Asteroid Deflection Research Center (ADRC), there has been a lot of research work done on the mitigation of near-Earth asteroids with short warning times (< 10 years) by studying potential mission designs to disrupt hazardous asteroids. The focus of this paper is on the determination/estimation of the orbital characteristics of near-Earth asteroids.

Techniques such as a high-precision gravitational simulator, encounter geometry, B-plane mapping, and gravitational keyholes are used in this paper to quantitatively evaluate the orbital characteristics of an asteroid and its associated impact risk. Using state information about the asteroid,

*Graduate Research Assistant, Asteroid Deflection Research Center, Department of Aerospace Engineering

†Vance Coffman Endowed Chair Professor, Asteroid Deflection Research Center, Department of Aerospace Engineering,

a high-fidelity gravitational model can be used to propagate the body into the future to see if and when it would come in close proximity to a planet, particularly Earth. These planetary encounters would change the asteroid's orbit, in shape and/or orientation. From the encounter geometry, the post-encounter heliocentric orbit of the asteroid could be in a resonance with that planet resulting in another encounter, or potentially an impact. Taking advantage of keyhole theory and the encounter's encounter plane, an estimate of the current and future impact probability of the asteroid can be made.

II. Background

A. Orbit Determination

The orbital motion of an asteroid is governed by a so-called Standard Dynamical Model (SDM) of the form [1]

$$\frac{d^2 \vec{r}}{dt^2} = -\frac{\mu}{r^3} \vec{r} + \sum_{i=1}^n \mu_i \left(\frac{\vec{r}_i - \vec{r}}{|\vec{r}_i - \vec{r}|^3} - \frac{\vec{r}_i}{r_i^3} \right) + \vec{f} \quad (1)$$

where $\mu = GM$ is the gravitational parameter of the Sun, n is the number of perturbing bodies, μ_i and \vec{r}_i are the gravitational parameter and heliocentric position vector of perturbing body i , respectively, and \vec{f} represents other non-conservative orbital perturbation acceleration.

The three most well-known orbital perturbations are solar radiation pressure (SRP), relativistic effects, and the Yarkovsky effect, the former two being the most prevalent effects. Solar radiation pressure provides a radial outward force on the asteroid body from the interaction of the Sun's photons impacting the asteroid surface. The SRP model is given by

$$\vec{a}_{SRP} = (K)(C_R) \left(\frac{A_R}{M} \right) \left(\frac{L_S}{4\pi cr^3} \right) \vec{r} \quad (2)$$

where \vec{a}_R is the solar radiation pressure acceleration vector, C_R is the coefficient for solar radiation, A_R is the cross-sectional area presented to the Sun, M is the mass of the asteroid, K is the fraction of the solar disk visible at the asteroid's location, L_S is the luminosity of the Sun, c is the speed of light, and \vec{r} and r is the distance vector and magnitude of the asteroid from the Sun, respectively.

The relativistic effects of the body are included because for many objects, especially those with small semimajor axes and large eccentricities, those effects introduce a non-negligible radial acceleration toward the Sun. One form of the relativistic effects is represented by

$$\vec{a}_R = \frac{k^2}{c^2 r^3} \left[\frac{4k^2 \vec{r}}{r} - \left(\dot{\vec{r}} \cdot \dot{\vec{r}} \right) \vec{r} + 4 \left(\vec{r} \cdot \dot{\vec{r}} \right) \dot{\vec{r}} \right] \quad (3)$$

where \vec{a}_R is the acceleration vector due to relativistic effects, k is the Gaussian constant, \vec{r} is the position vector of the asteroid, and $\dot{\vec{r}}$ is the velocity vector of the asteroid [3].

Taking into account these non-gravitational perturbations, the error within the system will increase, but their inclusion is needed in order to maintain consistency with the planetary ephemeris. A more complete dynamical model will allow the accurate calculation of asteroid impact probabilities and gravitational keyholes, leading to more effective mission designs. The gravitational model used in orbit propagation uses a variable stepsize Runge-Kutta Fehlberg (RKF) 7(8) method that takes into account the effects of the Sun, all eight planets, Pluto, the three largest main belt asteroids (Ceres, Pallas, Vesta), as well as solar radiation pressure and relativistic effects.

B. Encounter Geometry

The dynamical system under consideration in the given encounter geometry analysis consists of the Sun, a planet orbiting the Sun on a circular orbit, and an asteroid, viewed as a particle, that is on an eccentric and inclined orbit around the Sun that crosses the orbit of the planet. Assume the planet has an orbital radius of one and the gravitational parameter of the Sun is also one, and the asteroid has orbital elements $(a, e, i, \omega, \Omega)$. In order to have the asteroid cross the orbital path of the planet, the asteroid must meet the following criteria: $q < 1 < Q$, where q and Q are the perihelion and aphelion distances, respectively, of the asteroid. The frame of reference established for this analysis is centered on the planet, the x -axis points radially opposite to the Sun, the y -axis is the direction of motion of the planet itself, and the z -axis completes the right-handed system by pointing in the direction of the planet's angular momentum vector. The three most important orbital elements used in the analysis are the heliocentric orbital elements semi-major axis a , eccentricity e , and inclination i , of the approaching body [4].

Let $\mathbf{U} = (U_x, U_y, U_z)$ and U be the relative velocity vector and magnitude between the planet and the asteroid [4], defined as

$$U = \sqrt{3 - \left[\frac{1}{a} + 2\sqrt{a(1-e^2)} \cos i \right]} \quad (4)$$

$$U_x = U \sin \theta \sin \phi \quad (5)$$

$$U_y = U \cos \theta \quad (6)$$

$$U_z = U \sin \theta \cos \phi \quad (7)$$

where θ and ϕ define the angles that define the direction of U by

$$\phi = \tan^{-1} \left[\pm \sqrt{\frac{2a-1}{a^2(1-e^2)}} - 1 \frac{1}{\sin i} \right] \quad (8)$$

$$\theta = \cos^{-1} \left[\frac{1 - U^2 - 1/a}{2U} \right] \quad (9)$$

where θ may vary between 0 and π , and ϕ between $-\pi/2$ and $\pi/2$.

After the asteroid has an encounter with the target planet, the \mathbf{U} vector is rotated by an angle γ in the direction ψ , where ψ is the angle measured counter-clockwise from the meridian containing the \mathbf{U} vector. The deflection angle γ is related to the encounter parameter b by

$$\tan \frac{1}{2}\gamma = \frac{m}{bU^2} \quad (10)$$

where m is the mass of the planet, in units of the Sun's mass. The angle θ after the encounter, denoted by θ' , is calculated from

$$\cos \theta' = \cos \theta \cos \gamma + \sin \theta \sin \gamma \cos \psi \quad (11)$$

and, defining $\xi = \phi - \phi'$, we have

$$\sin \xi = \sin \psi \sin \gamma / \sin \theta' \quad (12)$$

$$\cos \xi = (\cos \gamma \sin \theta - \sin \gamma \cos \theta \cos \psi) / \sin \theta' \quad (13)$$

$$\tan \xi = \sin \psi \sin \gamma / (\cos \gamma \sin \theta - \sin \gamma \cos \theta \cos \psi) \quad (14)$$

$$\tan \phi' = (\tan \phi - \tan \xi) / (1 + \tan \phi \tan \xi) \quad (15)$$

Evaluating for the post-encounter variables θ' and ϕ' , the values of a' , e' , and i' can be obtained accordingly [4]. Figure 1 pictorially represents the relationship between the pre-encounter (U , θ , ϕ) and post-encounter (U' , θ' , ϕ') variables that make up the geometry of a body's encounter [4].

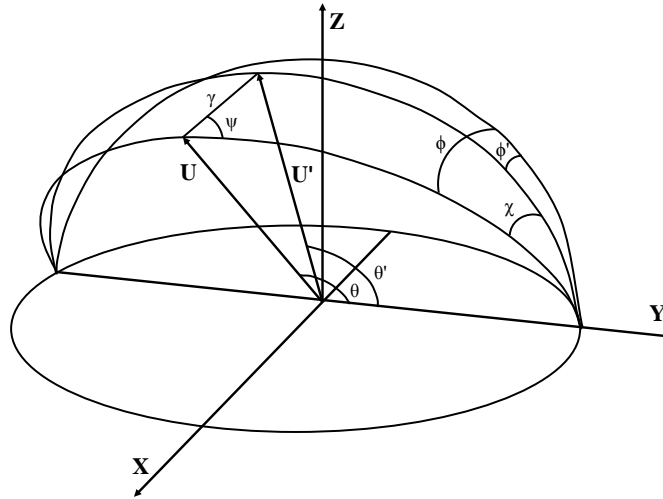


Figure 1. Reference frame of U and U' . After an encounter with a planet, the vector U is rotated by an angle γ in the direction of ψ .

C. Post-Encounter Orbital Analysis

Every encounter a body has with a planet results in an altered heliocentric orbital trajectory. The amount of the orbit change depends on the speed the body has relative to the planet and how close it gets, but it is possible to find the varied orbital trajectory of the body after encounter. Aside from using a high-precision propagation scheme to progress the body's state throughout the encounter, the encounter phase can be modeled as two-body motion governed by the planet as the central body.

Through an encounter with Earth, the incoming and outgoing v-infinity vectors and the pre- and post-encounter heliocentric velocities connect at the flyby planet through the following relationships

$$\vec{v}_{\infty}^{-} = \vec{v}_{\oplus}^{-} - \vec{v}^{-} \quad (16)$$

$$\vec{v}_{\infty}^{+} = \vec{v}^{+} - \vec{v}_{\oplus}^{+} \quad (17)$$

where \vec{v}_{∞}^{-} and \vec{v}_{∞}^{+} are the incoming and outgoing v-infinity vectors, respectively, \vec{v}_{\oplus}^{-} and \vec{v}_{\oplus}^{+} are the velocities of the flyby planet upon entry and exit of the planetary sphere of influence, and \vec{v}^{-} and \vec{v}^{+} are the heliocentric velocity vectors entering and leaving the sphere of influence of the planet, respectively [5].

The value of v-infinity is defined as

$$v_{\infty} = |\vec{v}_{\infty}^{-}| = |\vec{v}_{\infty}^{+}|. \quad (18)$$

So, the heliocentric speed gained by the body through the planetary encounter and the heliocentric delta-v vector caused by the flyby can be determined through the following two equations

$$\Delta v = 2v_{\infty}/e \quad (19)$$

$$\Delta \vec{v} = \vec{v}^+ - \vec{v}^- \quad (20)$$

where e is the eccentricity of the flyby hyperbola [5]. Numerically, the following nonlinear equality path constraint must be satisfied.

$$|\vec{v}_\infty^-| - |\vec{v}_\infty^+| = 0 \quad (21)$$

So, given the pre- and post-encounter heliocentric velocity vectors of the body, along with their respective heliocentric position vectors, the orbital elements of the heliocentric orbits can be found and compared to see just how much the orbit of the body has changed.

The data on orbital element variations through a planetary flyby can be used to also find resonance orbits between the body and the flyby target. The key parameter for resonant return orbits is the post-encounter semi-major axis. Assuming the flyby planet is the Earth, everything can be scaled so the Earth-Sun distance and the Sun's gravitational constant are equal to 1

$$T^2/a^3 \approx 4\pi^2 \quad (22)$$

where T and a are the period and semi-major axis of the body, respectively, in nondimensional units. Given that Earth's orbital period sweeps through an angle of 2π , the encountering body's post-encounter orbital period is $2\pi(a')^{3/2}$, where a' is the post-encounter semi-major axis. If the Earth and post-encounter body's periods are commensurable, then after h periods of the asteroid and k periods of the Earth have passed, where k and h are integers, a new encounter will take place as

$$(a')^{3/2} = k/h \quad (23)$$

Picking a number of Earth orbits to elapse, and an acceptable tolerance for the orbital ratio (k/h), the number of asteroid orbits can be found that would correspond to a resonance orbit existing between the asteroid and Earth from a given post-encounter semi-major axis.

D. B-planes and Keyholes

On any given encounter with a planet, the body passes through what is known as a target plane. On these target planes can exist what are called keyholes, and if the body were to pass through said keyhole, it would return on a resonant return orbit and impact the planet.

A target plane is defined as a geocentric plane oriented to be normal to the asteroid's geocentric velocity vector. In general, there are two distinct planes and several coordinate systems that can be used in such a framework. The classical target plane is referred to as the B-plane, which has been used in astrodynamics since the 1960s. The B-plane is oriented normal to the incoming asymptote of the geocentric hyperbola, or normal to the unperturbed relative velocity \vec{v}_∞ . The plane's name is a reference to the so-called impact parameter b , the distance from the geocenter to the intercept of the asymptote on this plane, known as the minimum encounter distance along the unperturbed trajectory [6]. Figure 2 depicts the relationship between the target B-plane and the trajectory plane of the asteroid.

One of the most important functions of the target plane is to determine whether a collision is possible, and if not, how deep the encounter will be. With the B-plane, the minimum distance of the unperturbed asteroid orbit at its closest approach point with the Earth can be determined - the impact parameter b . That single variable however does not tell whether the asteroid's perturbed trajectory will intersect the image of the Earth on the next encounter, however the information can

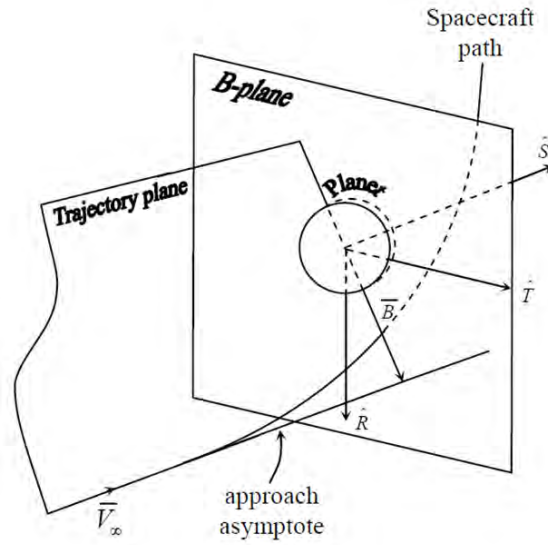


Figure 2. Representation of the target B-plane of a planet with respect to the incoming approach of a body on the trajectory plane.

be extracted by scaling the Earth radius R_\oplus according to the following relationship

$$b_\oplus = R_\oplus \sqrt{1 + \frac{v_e^2}{v_\infty^2}} \quad (24)$$

where v_e is the Earth escape velocity

$$v_e = \sqrt{\frac{2GM_\oplus}{R_\oplus}} \quad (25)$$

With this formulation a given trajectory impacts the Earth if $b < b_\oplus$, and would not otherwise [7].

A convenient and common target plane coordinate system (ξ, η, ζ) is obtained by aligning the negative ζ -axis with the projection of the Earth's heliocentric velocity \vec{V}_\oplus , the positive η -axis with the geocentric velocity (normal to the B-plane), and the positive ξ -axis in such a way that the reference frame is positively oriented, expressed as

$$\vec{\eta} = \frac{\vec{U}}{|\vec{U}|} \quad (26)$$

$$\vec{\xi} = \frac{\vec{\eta} \times \vec{V}_\oplus}{|\vec{\eta} \times \vec{V}_\oplus|} \quad (27)$$

$$\vec{\zeta} = \vec{\xi} \times \vec{\eta} \quad (28)$$

where \vec{U} is the geocentric velocity vector of the asteroid. With this reference frame, it can be seen that $\vec{\xi}$ and $\vec{\zeta}$ are on the B-plane itself, where (ξ, ζ) are the target plane coordinates that indicate the cross track and along track miss distances, respectively. That way, ζ is the distance in which the asteroid is early or late for the minimum possible encounter distance. The ξ coordinate, on the

B-plane, refers to the minimum distance achieved by altering the timing of the encounter between the asteroid and the Earth, known as the Minimum Orbital Intersection Distance (MOID). It is important to note that this particular interpretation of the coordinates of the B-plane is only reliable in the linear approximation, and unusable for distant encounters beyond several lunar distances.

A resonant return orbit is a consequence of an encounter with Earth, such that the asteroid is perturbed into an orbit of period $P' \approx k/h$ years, with h and k integers. After h revolutions of the asteroid and k revolutions of the Earth, both bodies are in the same region of the first encounter, causing a second encounter between the asteroid and the Earth. The term ‘keyhole’ is used to indicate small regions of the B-plane of a specific close encounter so that if the asteroid passes through one of those regions, it will hit the Earth on the next return. An impact keyhole is one of the possible pre-images of the Earth’s cross section on the B-plane tied to the specific value for the post-encounter semi-major axis that allows the subsequent encounter at the given date [6].

E. Impact Probability Calculation

One of the simplest ways, in theory not necessarily computationally, of calculating an impact probability of an asteroid and a planet is to simply divide the number of virtual asteroids that hit the planet, known as virtual impactors, by the total number of virtual asteroids used in the computation. The problem is that this method can be very computationally expensive, where the number of simulations needing to be run is approximately equal to the inverse of the impact probability [6].

The use of a statistical approximation can decrease the necessary number of simulations. To do this, a three-dimensional probability density function (PDF) of the asteroid’s close-approach position has to be found. So, the impact probability of 2012 DA14 becomes the triple integral of the PDF over the volume of the Earth. The expression can be simplified by making use of spherical coordinates.

$$IP = \int \int \int_{V_{\oplus}} PDF(x, y, z) dx dy dz \quad (29)$$

$$= \int_0^{r_{\oplus}} PDF(r) dr = CDF(r_{\oplus}) - CDF(0) \quad (30)$$

$$= \frac{1}{2} \left[erf \left(\frac{r_{\oplus} - \mu}{\sigma\sqrt{2}} \right) - erf \left(\frac{0 - \mu}{\sigma\sqrt{2}} \right) \right] \quad (31)$$

where CDF denotes the cumulative density function, μ is the mean distance from the Earth, σ is the standard deviation of the periaapse distances from the Earth, and r_{\oplus} is the radius of the Earth. This formulation results in a number between 0 and 1, corresponding to the probability of impact. Having a larger pool of virtual asteroids used in the computation increases the computation time, but should yield a more accurate impact prediction [2].

III. Example Orbital Simulation

Through the use of close encounter geometry, the variation in orbital elements between pre-encounter and post-encounter heliocentric orbits were calculated. Using those orbital variations potential orbital resonances between the asteroid and Earth were found. The concept of B-plane mapping enabled the construction of the asteroid’s encounter B-plane, which was used to ascertain the crossing points of virtual asteroids propagated through the B-plane. And using analytic keyhole

theory, along with the potential orbital resonances found, the location of keyholes on the encounter B-plane could be found. Finally, taking the B-plane crossings data and a statistical model for estimating impact probability, the impact probability of the asteroid was computed for the current encounter. The given algorithm yields a first-cut approximation of impact probability for near-Earth asteroids.

As an example asteroid, 2012 DA14 is analyzed using the aforementioned theory in [12]. On

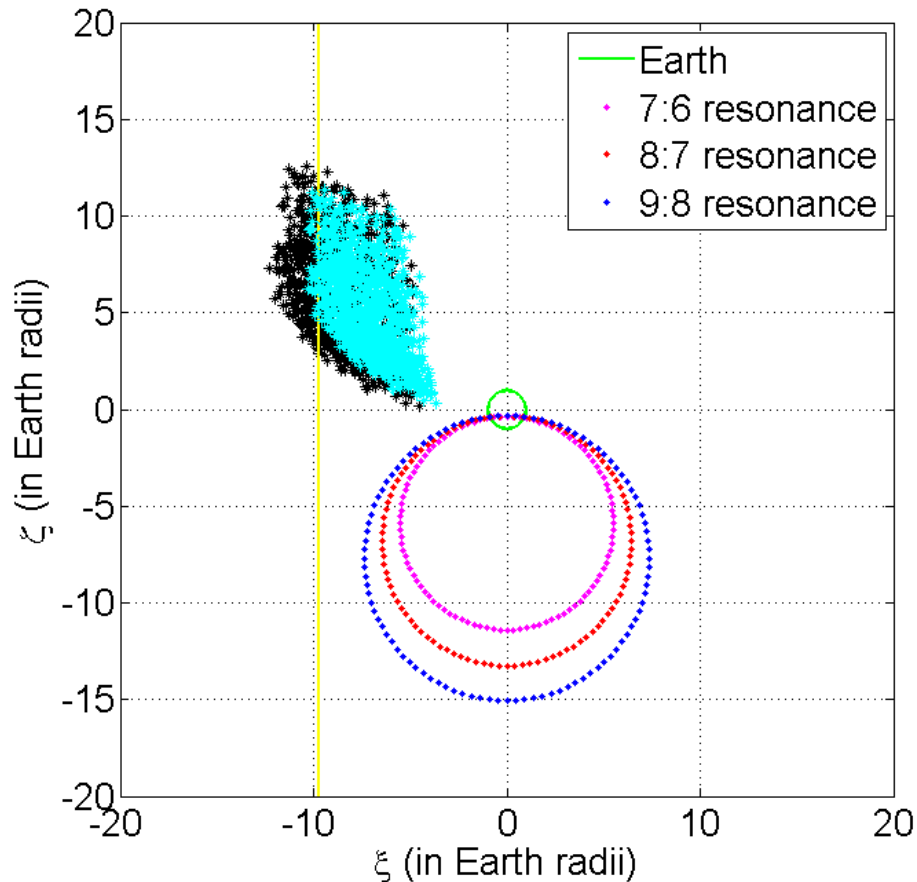


Figure 3. Encounter B-plane for February 2013 encounter of 2012 DA14 with Earth.

Figure 3, the green circle centered on the origin of the plot represents the projection of the Earth on the asteroid's B-plane. The purple, red, and blue circles represent 7:6, 8:7, 9:8 orbital resonances, respectively, for 2012 DA14 with Earth. The vertical yellow line on the B-plane represents the anticipated crossing of the asteroid, based on analytic keyhole theory. The distribution of cyan and black stars on the figure show the crossing points of the simulated virtual asteroids on the B-plane obtained via numerical integration and state transition matrix propagation.

For the analysis conducted, no keyhole existed on this B-plane and the only threat that existed from the body was the potential of an impact on the given encounter. The possibility of an impact on the current encounter was small however, about 0.02% [12]. The calculation of the impact risk of an asteroid potentially passing through a keyhole or having multiple encounters with the same body, such as Apophis or 2013 PDC-E (a fictitious asteroid created as an exercise at the 3rd Planetary Defense Conference in April 2013), having known keyhole properties has to be handled differently. This paper will go into the methodology of finding the probability of a keyhole passage

and the early detection of multiple encounters by an asteroid. More specifically, the paper explores the impact risk posed by a disrupted asteroid on route to Earth on both the current encounters of the fragments and the threat they hold in the near future (10 years).

IV. Potential Keyhole Passage

In the example orbital simulation shown previously, the process by which we assess the risk of an asteroid having an impact with the Earth, or any planet for that matter, was applied to asteroid 2012 DA14. The assessment of an asteroid's or asteroid fragment's potential for a resonant return after encountering a planet is a more challenging question to answer. A multitude of methods exist to answer that question, such as long-term orbital simulations tracking the asteroids or asteroid fragments or analytic keyhole theory to find the regions in an encounter B-plane that would result in a resonant return with the planet. Each method has a cost associated with it, the long-term orbital simulations can take a large amount of computation time but are fairly high-fidelity, while the analytic theory takes a significantly smaller amount of computation time while proving lower-fidelity results. Taking advantage of the semi-analytic protocol discussed in this paper, as stated in the introduction, can produce reliable results while not requiring a tremendous amount of computation time.

Looking back to Figure 3, it can be seen that no keyhole existed on the 2013 B-plane of 2012 DA14 that would result in a resonant return of the asteroid within the next 10 years. The evidence for the existence of such a region in the B-plane would be indicated by the intersection of the vertical yellow line and any one of the resonance circles. That intersection tells us that a keyhole exists in that region of space, but not the size of that keyhole. Because a keyhole is the projection of the Earth's future position on the current encounter B-plane, the shape of the keyhole closely follows the resonance circle, making it look like an arclet. That being said, given that each asteroid fragment is taken to be a point mass with no discernable size or shape, it would be difficult to assess the likelihood that any one fragment would actually pass through the keyhole, so instead of counting the number of fragments that would pass through that region and dividing by the number of total virtual fragments simulated, the area method for keyhole passage is constructed and employed to find the potential for a fragment to fall through that region of the encounter B-plane.

A. Area Method for Keyhole Passage Assessment

The virtual fragments constructed through the orbital uncertainty of a single asteroid fragment propagated through the encounter B-plane occupy a fraction of the B-plane's area. The keyhole on the same encounter B-plane also occupies a fraction of the B-plane area, however, not necessarily the same or even overlapping areas of the B-plane. This method claims no accuracy, only that it can be a way to quickly evaluate the risk potential of an asteroid and/or its fragments, and the method does not hold for instances where the keyhole region and the virtual fragment cloud region are too far removed from each other, where the keyhole passage probability would be assumed to be zero.

Consider the case where the keyhole region resides near the virtual fragment cloud of the asteroid fragment: how do we effectively evaluate the potential of the fragment to fall within the keyhole region? This question is answered using an area method that attempts to capture a majority of the virtual fragments within a bounding box and is proportional to the ratio of the area of the

keyhole region and the bounding box. The example presented here is only to show the methodology employed, it is not intended to describe an accurate, real-life scenario.

Assume that an asteroid has a virtual asteroid cloud, comprising of 10000 virtual asteroids, passing through the Earth's encounter B-plane such as that indicated by the blue stars and the red stars showing the position of the same virtual asteroid cloud on the next encounter B-plane in Figure 4. The yellow stars in each cloud indicate the virtual asteroids that pass within 1.1 Earth radii

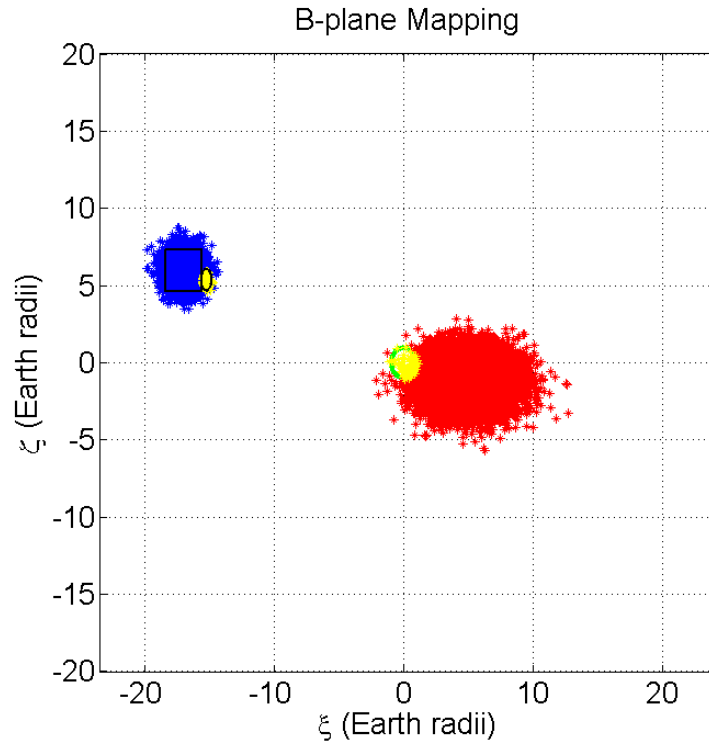


Figure 4. Example composite encounter B-plane for successive encounters of an asteroid with Earth.

radii on the second encounter B-plane. It is worth mentioning that the crossing points on the first encounter B-plane were created such that the probability of an impact with the planet on the first pass is zero. Before discussing the first encounter crossing point data, let's look at the second encounter data. Of the 10000 virtual asteroids, 66 fall within 1.1 Earth radii of Earth's surface on that particular encounter, making the impact probability for the encounter 0.66%. Using Eq. (29), the resulting impact probability is estimated to be about 0.71%, showing strong agreement between the statistical approximation established by Eq. (29) and the simulated results.

Now, let's look back to the first encounter crossing data, it can be seen that there is a black box and ellipse over the crossing point data. The box is constructed to have dimensions large enough to encompass at least 90% of the data points, and the ellipse is constructed with dimensions such that 95% of the data points fall within the prescribed area. The percentage values given are simply chosen to capture a large majority of the crossing points within each region and hold no special significance. When implemented using a simulated asteroid fragment, the dimensions of the keyhole region will be established based on the theory, so the proportion of the crossing points falling within the area will be simply the number within the region divided by the simulated fragments.

So, to construct the impact risk assessment for the asteroid based on its virtual asteroid field

$$IP = \left[\frac{A_{ellipse}}{A_{box}} \right] p_{box} p_{ellipse} (1 - p_{ellipse}) \quad (32)$$

where $A_{ellipse}$ and A_{box} are the areas of the ellipse and box encompassed by those shapes on the encounter B-plane, respectively, and p_{box} and $p_{ellipse}$ are the proportion of the crossing points that fall within the box and ellipse, respectively. With the resulting formula, the probability of an impact by the asteroid on its second encounter with Earth is evaluated to be about 0.5%.

Looking at the result, it is easy to see that it is not the same value as those found using either Eq. (29) or the simulated results on the second encounter B-plane crossing data. The results shouldn't be expected to be the same, or even necessarily in the same ballpark, because depending on the amount of time between encounters the field of virtual asteroids can disperse quite a bit leaving the impact probability on the second encounter plane to be essentially zero. As previously stated, this formula is not guaranteeing the accurate assessment of the impact probability of a body on future encounters, but is simply being used to find a solution so as to give an evaluation of whether or not the asteroid would need to be studied further.

V. Fragmented Asteroid Example

Keeping with the same asteroid example, 2012 DA14, let's assume that a mission was carried out to disrupt the asteroid in its orbit on October 1, 2012, about four and a half months before its anticipated encounter with Earth in the middle of February of 2013. The result of the disruption mission is 2012 DA14 becoming 21 pieces, 20 fragmented pieces of the asteroid and a piece that represents the original asteroid, still on a potential collision course with Earth. Even with the disruption of the asteroid body, the center of mass of the fragmented asteroids will still be on the same original orbit as the original asteroid. The fragments however, will have small deviations in their position and velocity from the original asteroid. With each fragment having a different state vector, every set of initial conditions is propagated from the initial epoch to encounter with the Earth's sphere of influence, or through a few days after the expected encounter date if the fragment doesn't cross the Earth's path. Each fragment has a 6-dimensional hypersphere margin of error as to its orbital position and velocity as it approaches Earth, so each fragment represents an orbital region where the fragment could actually reside in. To account for this orbital uncertainty, each fragment will be simulated by 1001 virtual asteroids about the fragment's orbital path.

To simulate the fragmentation of the asteroid body, a fragmentation model was created to add a certain amount of radial velocity to the asteroid fragments, as follows

$$\Delta v_i = \frac{\Delta v_{nominal} * r_i}{1 + (r_{max} - r_i)} \quad (33)$$

where Δv_i is the velocity added to the i^{th} fragment, $\Delta v_{nominal}$ is the desired amount of velocity to be added, r_i is the relative radius of the i^{th} fragment from the original asteroid's position, and r_{max} is the maximum radial distance of a fragment from the original asteroid's position after the fragmentation. The equation is an exponential decay function set up in such a way that the further the fragment is from the original asteroid position, the less radial velocity has been added to the fragment. Figure 5 shows the distribution of the asteroid fragment velocity additions using the above fragmentation model. After each fragment has had its fragmentation velocity added, the

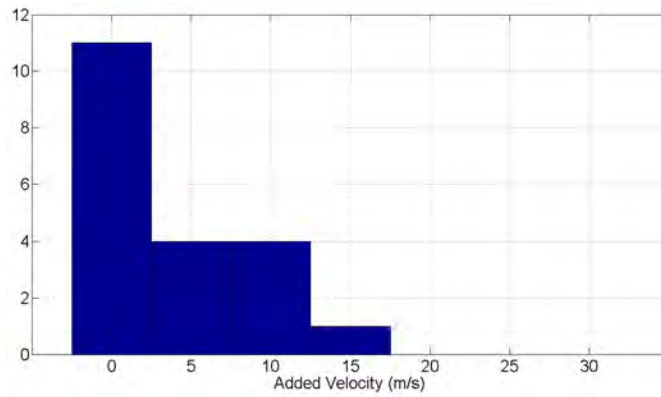


Figure 5. Histogram showing the distribution of the added velocity from the fragmentation to each asteroid fragment.

new states of the asteroids are created and propagated along their orbital paths. Figures 6 and 7 visually show the representative scattering of the asteroid fragments from the center of mass of the original asteroid and a cross-section of the fragment cloud on a collision course with Earth on the approach trajectory of the asteroid.

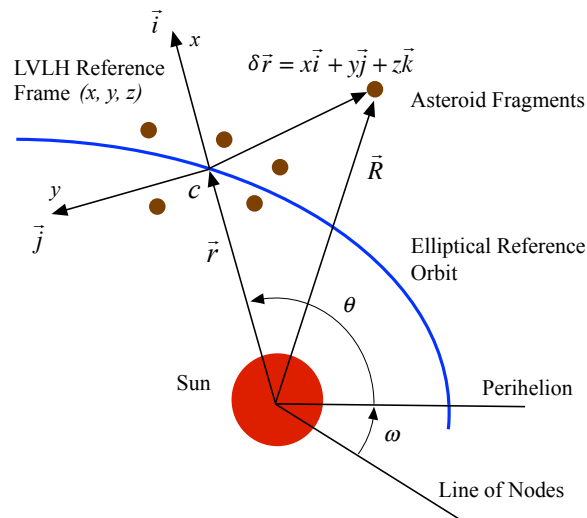


Figure 6. Depiction of the relative position of the asteroid fragments to the asteroid's original position/fragments' center of mass.

Before getting into the analysis of the fragments and their encounters, or lack thereof, with the Earth, there is one thing that is important to keep in mind at this point. With the simulated fragmentation of asteroid 2012 DA14, used an example to develop the computational tool being discussed in this paper, each fragment now has a different state vector (position and velocity state) than the original asteroid, therefore in the analysis conducted here each fragment is considered to be its own “new” asteroid and is treated as such. With that said, again there are assumed to be 21 equal sized pieces of the original asteroid after the fragmentation event. Each piece of the asteroid has two possible outcomes for its approach trajectory, either the fragment will cross into the Earth’s SOI and have an encounter with the planet, or it will miss the SOI and continue on its path without much influence from the Earth. Given this simulation, it happens that one of

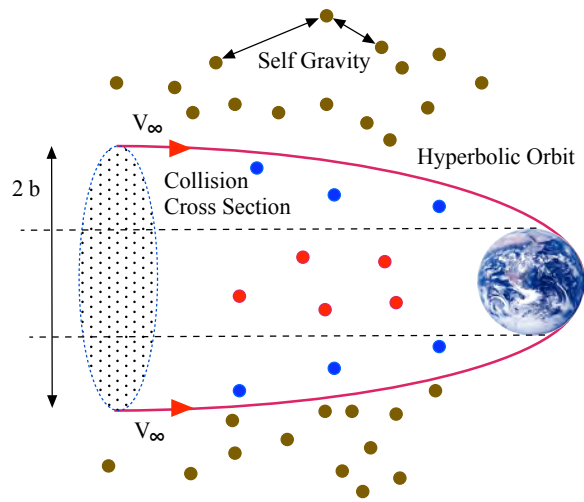


Figure 7. Collision cross-section of the asteroid fragment cloud.

the fragments doesn't encounter the Earth's SOI, meaning that the fragmentation has successfully dismissed one of the 21 asteroid pieces. That one fragment would have to be monitored to make sure that it wouldn't come back in the future, but for this analysis we assume that it doesn't have any future encounters with the planet. The remaining 20 pieces have some kind of encounter with the Earth, and Figure 8 shows the distributions of the asteroid fragment's orbital elements. Looking

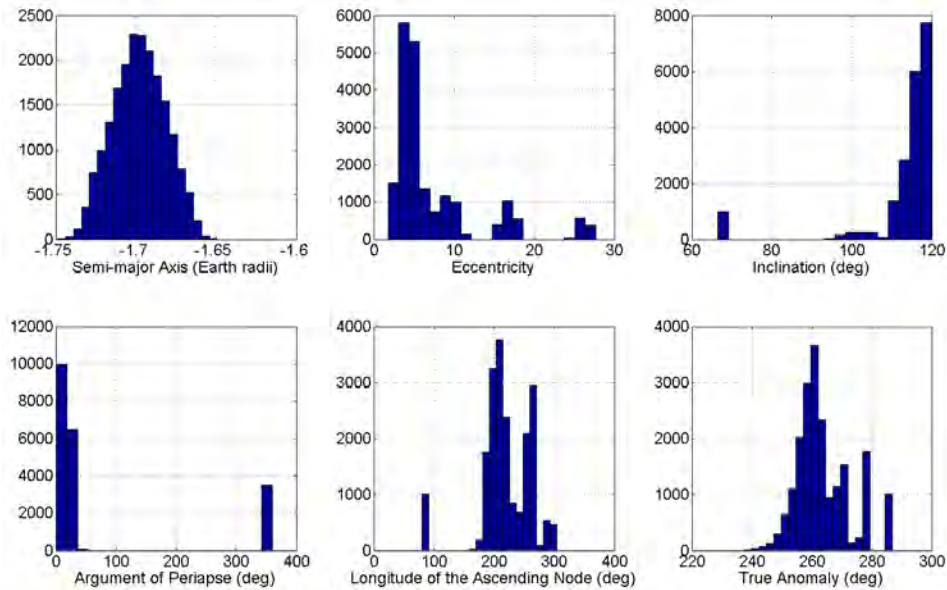


Figure 8. Histogram showing the distribution of the fragment clouds upon entering the Earth's sphere of influence.

at all the distributions of orbital elements for all the encountering fragment's clouds it can be seen that the asteroid fragments will have various kinds of encounters with the Earth. Therefore, it would be expected that the fragment clouds would have crossing points spread across the B-plane, rather than centrally located like in the example of the nominal trajectory of 2012 DA14 .

A. Fragment Analysis

Figure 9 shows a composite B-plane of all the encountering asteroid fragments with Earth to show how the pieces could end up dispersing after the given fragmentation. The green circle represents

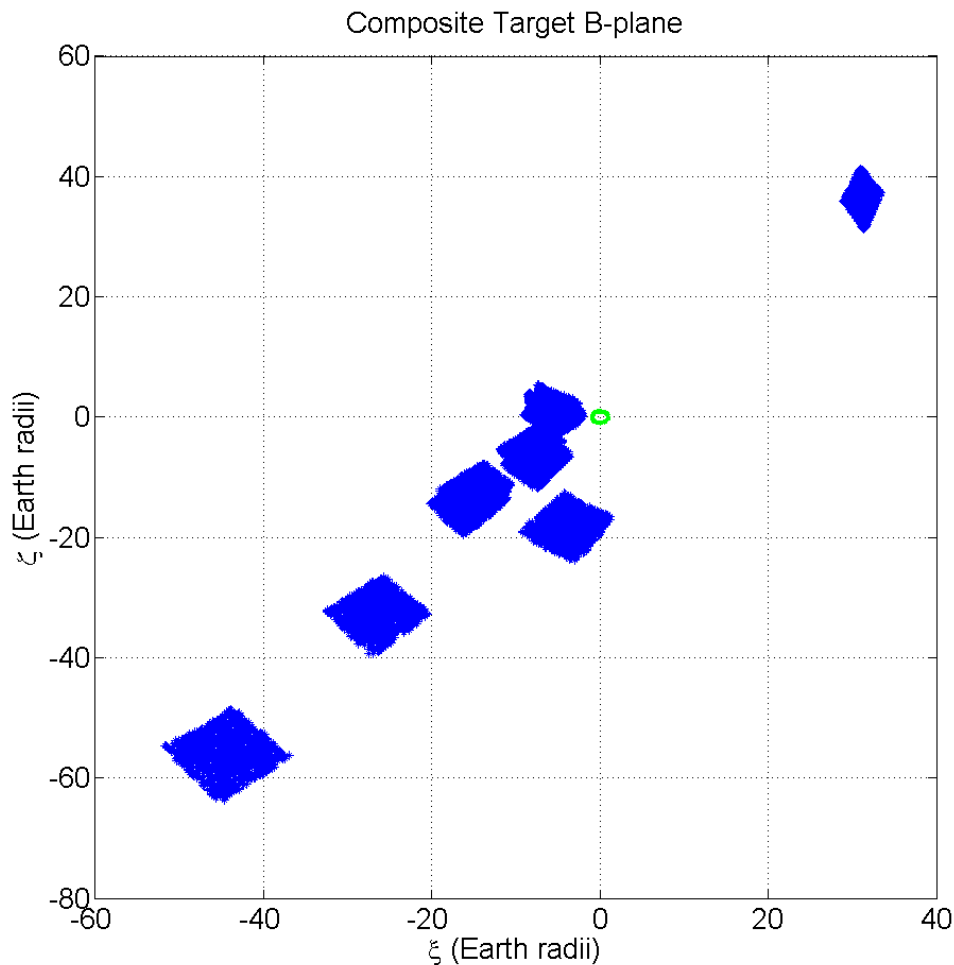


Figure 9. Composite B-plane of all the encountering asteroid fragment fields.

the Earth's cross-section on the B-plane, and the blue stars represent the various fragment fields of the asteroid fragments. It is easy to see how the added velocity from the fragmentation has caused some of the fragment clouds to drift away from the Earth in the B-plane.

Now looking back at Figure 3, the reader will recall that each encounter with a planet there are potential resonances that the body can fall into after the encounter, in addition to the potential that the asteroid can impact the planet on the current encounter. So, there are four categories that any given asteroid encounter can fall into: (1) impact and resonance potential, (2) impact and no resonance potential, (3) resonance and no impact potential, and (4) no resonance or impact potential. Even with the relatively small number of asteroid fragments simulated, there is a representative fragment for each of these four groups. Therefore, instead of talking about the larger picture, which can get convoluted due to the number of particles and number of potential resonances for the fragmented asteroids, an analysis will be given of an asteroid fragment in each group and all other fragments can be assumed to fall into one of the four groups.

1. Impact and Resonance Potential

For the first case, the asteroid fragment to be looked at is one that has an impact risk on the first encounter with Earth and a potential for a resonant return impact encounter in the future. As can be seen in Figure 10, where the red dots show the crossing points of the fragment field and the green circle indicating the location of the Earth, this fragment turns out to have a small, but non-zero, impact probability with the Earth on its first encounter. Using Eq. 29, the estimated impact probability of this fragment is about $2.17\text{E-}14$, so small that it has virtually no chance of impacting the planet on this first encounter. The significance of this particular fragment field is not in its small impact potential, but in its resonance potential. Looking closely at the figure, it can be seen

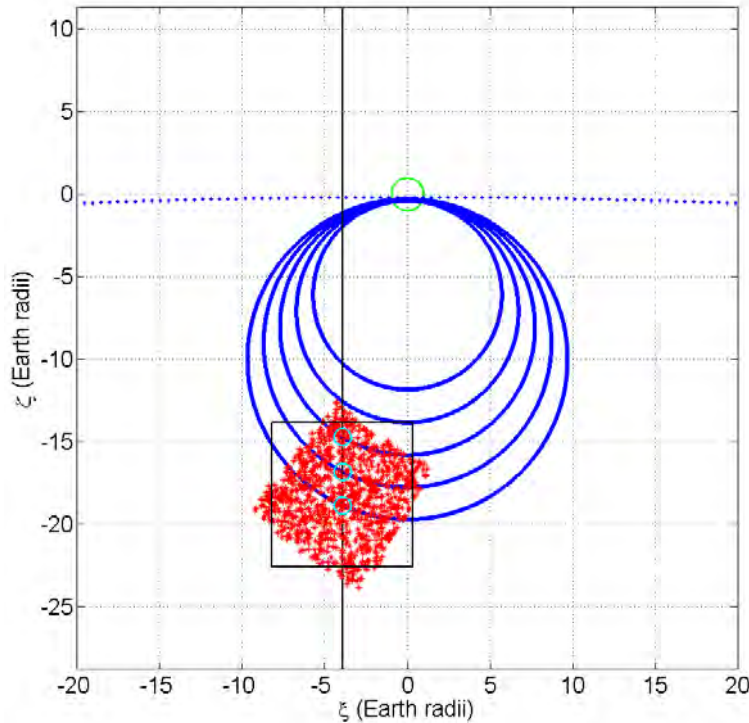


Figure 10. B-plane of an asteroid fragment that has potential to impact the Earth on the original encounter and has a potential for a future resonance encounter.

that there are six potential Earth resonances based on the fragment's simulated encounter with the Earth. And, according to the analytic keyhole theory described earlier, the intersections between the vertical black line in the figure and the blue resonance circles indicate locations where keyholes may exist on this target B-plane. Given the clustering of the fragment field, the three cyan circles encompass the locations where a keyhole could exist. The other intersection points could also have keyholes associated with them, but they are not looked at based on the location of the fragment field's crossing points.

It is worth noting at this point, that the size and shape of these cyan circles do not reflect the size and shape of keyholes based on the analytic theory. The analytic theory says that the width of a given keyhole is approximately $2b_{\oplus}$ and has a maximum width that is dictated by the ratio of the resonance circle. The cyan circles are being used to show a region where if the asteroid fragment would pass through could result in an impact or at least very deep future orbital encounter. The probability of having the asteroid fragment pass through a given cyan circle in Figure 10 is

calculated using Eq. 32. Going from the top down, the probability that the fragment passes through the cyan circles on the target B-plane is 0.0054%, 0.0031%, and 0.0054%, respectively. Again, these probabilities are extremely small, but maybe not necessarily small enough to ignore. If the probabilities are found to be large enough that they are worrisome, a more refined study can be done with larger fragment fields and/or using a long-term precision propagator to find the true potential and depth of any future encounters. However, for this study, this particular fragment field shows the capabilities of this analysis tool to find a relatively quick and robust solution to the current and future impact risk.

2. *Impact and No Resonance Potential*

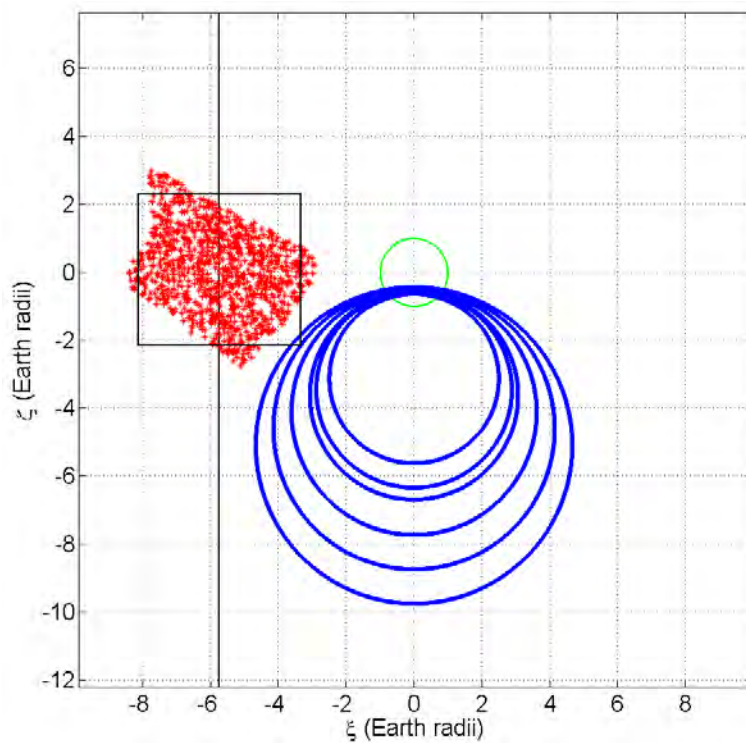


Figure 11. B-plane of an asteroid fragment that has potential to impact the Earth on the original encounter and has no potential for a future resonance encounter.

Let's now look to a fragment that has a potential to impact the planet on its first encounter, but does not appear to fall into a resonance orbit with Earth within the next 10 years. In Figure 11, the fragment field passes a lot closer to the planet than the field depicted in the Impact and Resonance Potential example. The impact probability of this particular field is estimated to be 0.000081%. This impact probability is much larger than in the previous example, but still fairly small and much smaller than that of the original asteroid. No resonance is said to exist between this fragment and the Earth because the multiple resonance circles shown on the target B-plane do not intersect the black, vertical line. Without that intersection, the analytic theory states that there is no existing keyhole on the plane for that kind of resonance orbit. That does not however mean that no keyhole exists on this particular B-plane, but there would be no way to find said keyhole without conducting an analysis of the fragment cloud via a high-fidelity numerical propagation scheme from the current

encounter to a given point in the future. So based on the mix of analytic and numerical techniques used through this analysis this fragment is deemed to be a small threat to the Earth on its current encounter, and no threat in the near future.

3. Resonance and No Impact Potential

The asteroid fragment used as a representative of the group that can fall into resonance orbits while having no chance of impacting Earth on their current encounter is rather harmless. Based on the analysis, Figure 12 clearly reinforces the lack of a threat posed by this fragment field. The red

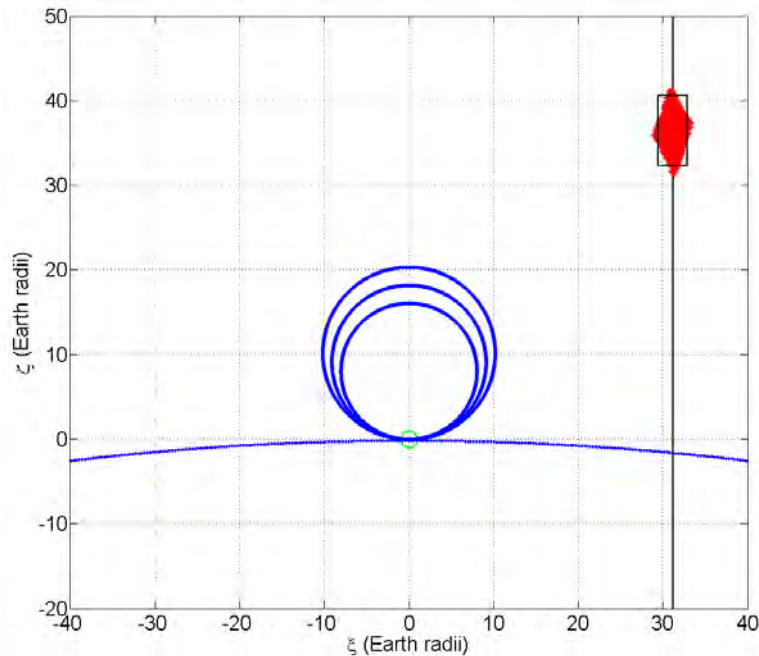


Figure 12. B-plane of an asteroid fragment that has potential to has a potential for a future resonance encounter and no impact potential on the current encounter.

dots that represent the crossing points of the fragment field are about 35 Earth radii from Earth, so calculating the impact probability on this encounter of this fragment field doesn't require the use of Eq. (29), but is found to be zero. In addition to the lack of impact risk on this encounter, there is no chance of the fragment to fall into a resonant return orbit after this Earth encounter. Of the four resonance circles shown in Figure 12, only one resonance circle intersects the black, vertical line - only one of those intersections is shown in the figure. The fragment field crosses the B-plane far from that intersection point where the keyhole would exist, so the probability of the fragment passing through that keyhole is presumed to be zero. However, if the timing of the fragment field crossing the B-plane were earlier than what it turned out to be, that fragment field would drift further down that black, vertical line and the possibility of the fragment passing through the corresponding keyhole and making a resonant return to Earth would go up.

4. No Resonance or Impact Potential

The last type of encounter that an asteroid fragment could have with Earth is one where there is no threat to the Earth on the current encounter or in the near future. This would be the category where

we would hope a large majority of asteroid fragments after a fragmentation event would end up, but whether that would be reality or not would depend on the effectiveness of the fragmentation and the resulting states of the fragments. The representative asteroid fragment of this group has

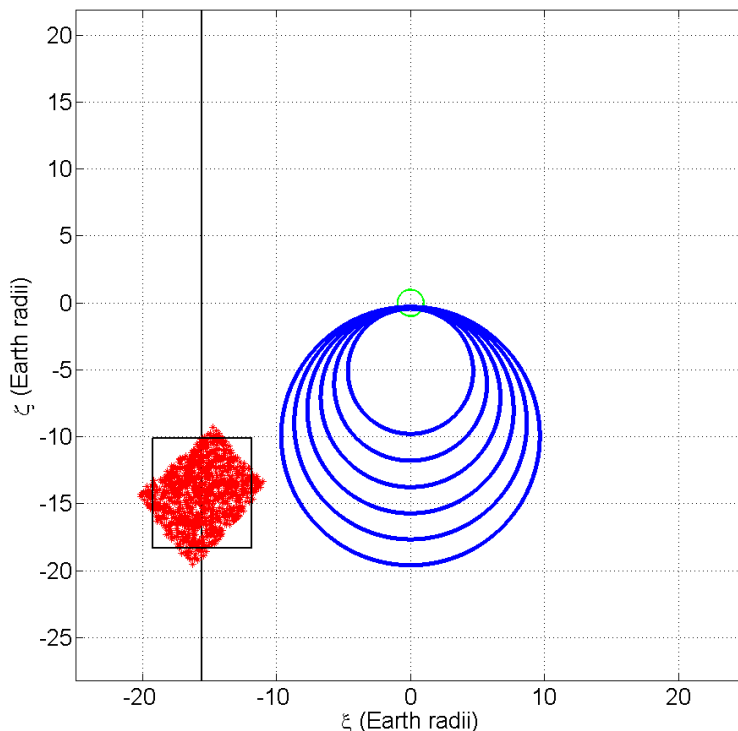


Figure 13. B-plane of an asteroid fragment that has no potential to impact the Earth on the original encounter or on any future resonance encounter.

its fragment field crossing the encounter B-plane on average about 21 Earth radii from the planet, so the estimated impact probability for this fragment is zero. Figure 13 shows that there are six resonance circles on the encounter B-plane, meaning there exist six potential resonances for the fragment after this encounter, but because none of these resonance circles intersect the black, vertical line for this fragment there are again no analytically defined keyholes on this fragment’s B-plane. Therefore, there is no chance of a resonant return for this fragment in the near future, implying no chance of a future impact during that period of time from this fragment.

VI. Conclusion

To this point the analysis of the impact risk posed by the asteroid fragments to the Earth on the original or later encounters has been looked at on an individual fragment basis. However, it would be nice to know the risk that the field possesses. Before we look into the field as a whole, let’s look back at the asteroid fragment used in the section relating to fragments that have both Impact and Resonance Potentials. That asteroid fragment had three identified keyholes that the fragment could pass through, each with its own keyhole passage probability. If we wanted to know the probability that the fragment would pass through any of the three given keyhole regions we calculate the union probability of these many independent events. The formulation for this union probability is fairly

simple, but gets more complicated the more independent events are included, is as follows

$$P(1 \cup 2 \cup 3) = P(1) + P(2) + P(3) - P(1 \cap 2) - P(1 \cap 3) - P(2 \cap 3) + P(1 \cap 2 \cap 3) \quad (34)$$

where $P(n)$ is the probability of the n^{th} event, $P(n \cap m)$ is probability of the intersection of the n^{th} and m^{th} , and $P(n \cup m)$ is the probability of the union of the n^{th} and m^{th} events. And, because the events are considered independent, the probability of the intersections of the events are defined as the product of the individual events. The calculated probability of the fragment passing through any of the three defined keyholes is 0.0014%, which is less than the probability of the asteroid passing through an individual keyhole.

Looking at the estimated impact probability of the fragment clouds on their first encounters with the Earth, the probabilities are fairly varied, as shown in Figure 14. As a reminder, the

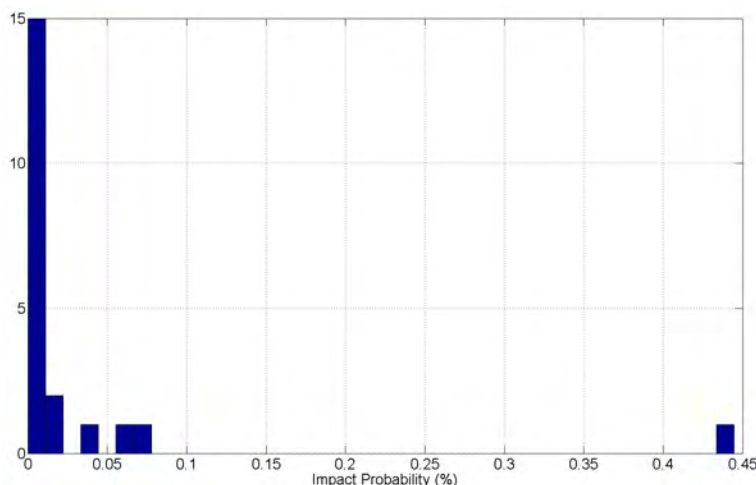


Figure 14. Distribution of the estimated impact probabilities of the asteroid fragments on their first (current) encounter with the Earth.

estimated impact probability of the asteroid on its original trajectory was about 0.02%. Most of the fragments have estimated impact probabilities that are less than that of the original asteroid, but there are a few that have probabilities that are greater. By expanding Equation (34) to take into account 21 independent events, one event for each asteroid fragment, the estimated probability that any given fragment would impact the Earth is extremely small, virtually zero.

Therefore, even with a fairly simple fragmentation of an asteroid that breaks up the asteroid into relatively few pieces and only adds a small amount of speed to the fragments (on the order of 5-20 meters per second), the impact risk posed by the fragment field is smaller than that of the original asteroid on its nominal trajectory. Note, this is not a universal claim, there can be certain types of fragmentations that could result in a larger impact risk to the Earth by the fragment field. Several types of fragmentation models can be implemented to see if a particular type of fragmentation is better than another, but what would be more useful would be an accurate simulation of the expected fragmentation of a given asteroid, composed of a certain type of material, with this kind of impact, this much energy introduced to the system, utilizing real-world phenomena. Those topics are beyond the scope of this paper, but are topics that should be looked into in the future before an actual asteroid fragmentation mission is proposed and launched.

This paper has shown the use of a developing protocol that can categorize the type of encounter those fragments can have by showing a representative fragment from those groups and assess the

risk posed by each fragment and of the fragments as a whole. The use of 2012 DA14 and its close-encounter with Earth in February 2013 is an example to show the capabilities of this protocol. We have shown the ability to identify the potential for a fragment to impact the Earth on its current encounter with the planet and the potential for it to pass through a region of the B-plane that theory tells us should lead to a future impact or at least another close encounter. Use of this protocol is intended to quickly evaluate the associated threat of a fragmented so that further study can be conducted if need be.

Acknowledgments

This research has been supported by a NIAC (NASA Innovative Advanced Concepts) Phase 2 study entitled “An Innovative Solution to NASA’s Asteroid Impact Threat Mitigation Grand Challenge and Its Flight Validation Mission Design.”

References

¹Chodas, P. W. and Yeomans, D., “Orbit Determination and Estimation of Impact Probability for Near Earth Objects,” AAS 09-002, *AAS/AIAA Space Flight Mechanics Meeting, 2009*.

²Pitz, A., Teubert, C., and Wie, B., “Earth-Impact Probability Computation of Disrupted Asteroid Fragments Using GMAT/STK/CODES,” AAS 11-408, AAS/AIAA Astrodynamics Specialist Conference, Girdwood, AK, August 1-4, 2011.

³Yeomans, D. K., Chodas, P. W., Sitarski, G., Szutowicz, S., and Krolikowska, M., “Cometary Orbit Determination and Nongravitational Forces,” *Comets II, The Lunar and Planetary Institute, 2004*, pp. 137-152.

⁴Carusi, A., Valsecchi, G. B., and Greenberg, R., “Planetary Close Encounters: Geometry of Approach and Post-Encounter Orbital Parameters,” *Celestial Mechanics and Dynamical Astronomy*, Vol. 49, 1990, pp. 111-131.

⁵“Gravity Assist Interplanetary Trajectories.” *Welcome to the Orbital and Celestial Mechanics Website*, C. David Eagle, 9 Dec. 2012. Web. 4 Dec. 2013.

⁶Milani, A., Chesley, S. R., Chodas, P. W., and Valsecchi, G. B., “Asteroid Close Approaches: Analysis and Potential Impact Detection,” *Asteroids III, The Lunar and Planetary Institute*, p. 55-69, 2002.

⁷Valsecchi, G. B., Milani, A., Chodas, P. W., and Chesley, S. R., “Resonant Returns to Close Approaches: Analytic Theory,” *Astron. Astrophys.*, 2001.

⁸Born, George H., “Design of the Approach Trajectory: B-plane Targeting,” ASEN 5519: Interplanetary Mission Design, University of Colorado at Boulder, 2005.

⁹Bourdoux, Arnaud. “Characterisation and Hazard Mitigation of Resonant Returning Near Earth Objects: The Case of 2004 MN,” Diss. Universite De Liege, 2004.

¹⁰*Near-Earth Object Program*, Ed. D. Yeomans, National Aeronautics and Space Administration. <http://neo.jpl.nasa.gov/index.html>.

¹¹Yeomans, D., Bhaskaran, S., Chesley, S., Chodas, P., Grebow, D., Landau, D., Petropoulos, A., and Sims, J., “Report on Asteroid 2011 AG5 Hazard Assessment and Contingency Planning.” *Near-Earth Object Program*. Ed. D. K. Yeomans, National Aeronautics and Space Administration. <http://neo.jpl.nasa.gov/index.html>.

¹²Vardaxis, G., and Wie, B., “Impact Probability Analysis for Near-Earth Objects in Earth Resonant Orbits,” AAS 14-427, AAS/AIAA Space Flight Mechanics Meeting, Santa Fe, New Mexico, January 26-30, 2014.